HYDRODYNAMIC DRIVERS OF SEDIMENT TRANSPORT ACROSS A FRINGING REEF

Willem Bodde[1], Andrew Pomeroy[2], Ap Van Dongeren[3], Ryan Lowe[2] and Jaap van Thiel de Vries[4,5]

Coral reefs are highly valuable ecosystems, which are under an increasing number of environmental pressures. Sedimentation and sediment transport patterns are among key physical drivers of coral reefs, so it is important to improve our understanding of these poorly studied dynamics on reefs. To this purpose, flume experiments were performed on a scaled fringing reef in the laboratory facilities of Deltares in Delft. The objective was to improve the understanding of hydrodynamic and sediment transport processes across fringing reefs. The water depth and bed roughness were shown to have influence on many processes such as short wave breaking, infragravity (IG) wave generation, IG wave transformation, reef flat seiching, wave-induced setup and wave reflection. The measurements showed that long waves dominate over the short waves at the back of the reef flat. The flow velocities in the rough cases were lower than those in the smooth cases as a result of the bed friction. Analysis of the third order velocity moment and the bed level changes indicates that both the short and the long waves play a role, but that the long waves appear to be the dominant factor in sediment transport and bed profile development - especially close to the beach. Bed roughness affected the shape of a swash bar, which was more pronounced for the smooth than for the rough cases. This demonstrates that the dominance of long waves in a fringing reef lagoon results in different sediment dynamics than, for example, on a regular sandy beach.

Keywords: fringing reef, sediment transport, infragravity waves, flume experiment, hydrodynamics, morphodynamics, seiching, bed friction, wave setup

INTRODUCTION

Background

Fringing coral reefs are natural structures located along stretches of coast in tropical and subtropical waters. These reefs are typically characterised by a steep forereef slope coming from deep water on the seaward side, with the crest of the reef usually around or just below mean sea level. A wide reef flat usually connects the crest with a lagoon that, if present, is sometimes deeper. Ecologically, reefs provide a strongly varied habitat and a diverse ecosystem; however they also protect the coast and beaches behind them by dissipating a large proportion of the incoming wave energy, acting as a natural breakwater (Ferario et al., 2014).

Many of the nearshore hydrodynamic studies to date have focused on sandy beaches with mild slopes and smooth beds (Komar, 1998). However significant progress has been made in understanding hydrodynamic processes in reef environments (see Monismith (2007) and Lowe et al. (2014) for recent reviews). As waves propagate over a reef they experience strong attenuation due to wave breaking and bottom friction (Lowe et al., 2005; 2007). The resulting change in radiation stress has been shown to cause a significant setup of the mean water level on the reef (Munk and Sargent, 1948; Young, 1989) and drives circulation within the reef system (Lowe et al, 2009). In addition to the setup, wave energy is redistributed across all frequencies and increases primarily in the low frequency range (Young, 1989; Lee and Black, 1978). The source of the redistribution of energy towards the lower frequency appears to be similar to surf beat generation mechanisms observed elsewhere.

This ‘surf beat’ is generated by the variation of wave height and therefore radiation stress under wave groups with waves of different frequencies. The variation causes a small setdown of the water level under the higher waves in the group and a small setup under lower waves. This creates a long wave that travels with, and is bound to, the wave group (Longuet-Higgins & Stewart, 1962; 1964). These long waves are released from the wave group at the short wave breakpoint and propagate towards the beach as free long waves where they reflect and propagate back in a seaward direction.

The generation mechanism of freely propagating long waves, or infragravity (IG) waves, in the nearshore is particularly strong for beaches with mild slopes and mild wave conditions (low short wave steepness) (Baldock, 2012). However, on steep slopes IG waves can be generated by a breakpoint mechanism as proposed by Symonds et al. (1982). According to this theory, long waves are generated by the temporal variation in the breakpoint location of the short waves that travel in groups. The breakpoint moves up and down in onshore and offshore direction because the higher waves break

[1] Witteveen+Bos, Rotterdam, The Netherlands (former: Deltares and TU Delft)
[2] University of Western Australia, Crawley, WA, Australia
[3] Deltares, Delft, The Netherlands
[4] Department of Civil Engineering, TU Delft, Delft, The Netherlands
[5] Boskalis, Papendrecht, The Netherlands (former: Deltares)

farther offshore than the lower waves in a group. The moving breakpoint causes a varying forcing on the water column, which behaves like a wave maker and thus generates waves at the group period and its harmonics. This was demonstrated for a reef by Pomeroy et al. (2012) using results from a field study and numerical modelling using XBeach (Roelvink et al., 2009).

On the reef flat and within the lagoon, the IG waves play an important role (Lee and Black, 1978; Young, 1989; Pomeroy et al., 2012). Van Dongeren et al. (2013) demonstrated that within Ningaloo Reef in Western Australia, the bottom shear stress attributed to IG waves accounted for up to 50% of the total shear stress and therefore it dominates over shear stress generated by short waves (<40%) and mean currents (up to 20%). It was also shown that bottom friction dissipation is much lower for IG waves than for short waves and the presence of IG waves is strongly modulated by the tide, mostly due to friction dissipation rates varying with the water level.

In comparison to the growing number of reef hydrodynamic studies, much less research has been done in the area of morphodynamics and sediment transport on and behind a coral reef. Yet sediment suspension and transport has been recognised to have a significant impact on coral reef ecosystems. High sediment concentrations and the resulting turbidity can lead to decreased light availability for photosynthesis eventually leading to coral mortality (e.g. Storlazzi et al., 2009). The accumulation of sediment at certain locations may stress the corals and coral colonies can be buried.

With high roughness values, steep slopes and IG motions dominating the bed shear stress over the flat, the dominant hydraulic processes on a coral reef are different than those on sandy beaches.

In this study we present the results of a laboratory experiment that was undertaken to investigate hydro- and sediment dynamics on a scaled fringing reef model with the aim to understand the hydrodynamic processes that drive sediment transport in reef environments. The study is part of a larger research program by the University of Western Australia into fringing coral reef hydro- and sediment dynamics (Pomeroy et al., in prep). The flume experiments were also modelled numerically with XBeach, showing good results and can be found in Bodde (2013).

This paper begins with a short description of the laboratory experiment (setup, measurements, case overview). Next the methods to analyse the data from the experiments are discussed. The paper focuses on analysis of the hydrodynamic data obtained from the experiments and subsequently discusses the implications for sediment transport. Data from bed profile measurements in the flume is then used to find how the bed profile has developed as a consequence of the hydrodynamics and the resulting sediment transport.

EXPERIMENTS

The experiments were performed on a scale 1:15 fringing reef model in the Eastern Scheldt Flume (Deltares). The flume dimensions were 55 x 1 x 1.2 m (LxBxH) and the wave generator is equipped with second-order (Stokes) wave generation and Active Reflection Compensation. The shape and dimensions of the reef, some terminology and the conditions used are presented in Figure 1.

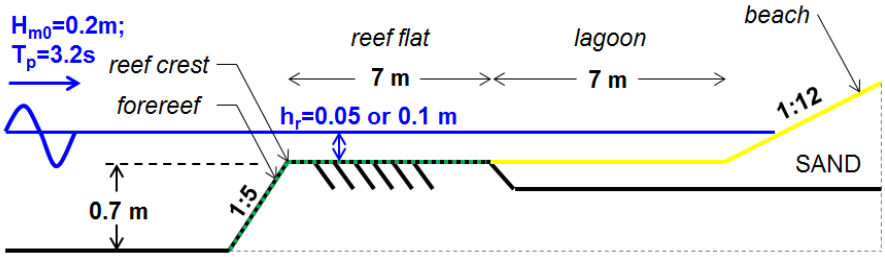

Figure 1. Experiment setup and hydrodynamic conditions

Four simulations with a duration of seven hours were performed: with and without roughness on the forereef and reef flat (green dashed area), and 5 cm ('deep') or 10 cm ('shallow') still water level (S10, S05, R10, R05). A repeating ten-minute TMA-type wave spectrum[6] with a significant wave height H_{m0} of 0.2 m (prototype 3 m) and a peak period T_p of 3.2 s (prototype 12.4 s) was used to generate the waves in the flume. The bed roughness was created by gluing concrete cubes of 1.8 cm length to smooth plywood covers while the lagoon and beach area had a movable sandy bed (D_{50}=115µm).

[6] The TMA spectrum is a variation on the JONSWAP spectrum with a more generalised applicability from deep water to arbitrary-depth water (Holthuijsen, 2007)

Measurements of surface elevation, flow velocity, suspended sediment concentration and bed profile development were obtained across the entire reef model. The measurements of the suspended concentrations are outside the scope of this paper and will be discussed in a paper by Pomeroy et al. (in prep.)

18 wave height meters (WHM) and 6 electromagnetic flow velocity meters (EMS) measured the hydrodynamic conditions while a custom made 3D profiler from Deltares was used to measure the cross-shore profile of the beach and the lagoon. Profile measurements were obtained before each run and at t = 1h, 3h and 7h. The strongest morphological developments were expected in the first hours, so the first profiles are taken at shorter time intervals. The location of the instruments is shown in Table 1 and Figure 2.

Table 1. Location of instruments in the flume

Location	X [m]	Wave height	Flow velocity	Position w.r.t. reef
1	16.28	X	X	Offshore
2	26.04	X	-	
3	28.24	X	-	Forereef slope at x=27.84-31.34
4	29.54	X	X	
5	30.24	X	-	
6	30.84	X	-	
7	31.11	X	-	
8	31.30	X	-	
9	31.69	X	-	Reef flat at x=31.34-38.34
10	32.34	X	X	
11	32.94	X	-	
12	34.24	X	-	
13	35.59	X	X	
14	37.14	X	-	
15	40.14	X	X	Lagoon with sandy bed at x=38.34-45.34
16	41.88	X	-	
17	43.63	X	X	
18	45.33	X	-	

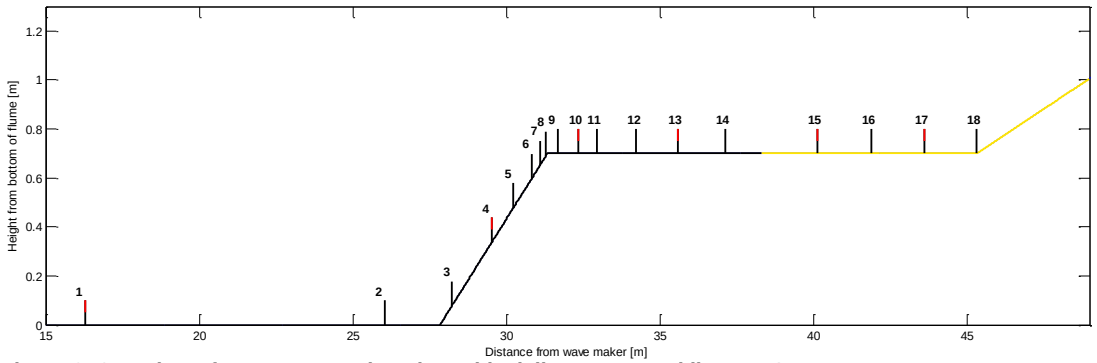

Figure 2. Overview of measurement locations; black line: WHM; red line: EMS.

METHODS

Spectral analysis

To analyse the wave transformation on the reef for different frequencies, the waves were separated by frequency; waves with a frequency higher than half the peak frequency are considered short waves ($f>f_p/2$, SW), waves with a frequency smaller than half the peak frequency are considered long waves ($f<f_p/2$, LW). The long wave frequency band was decomposed (by bandpass filtering) into infragravity ($0.025 \text{ Hz} < f < f_p/2$, IG) and very low frequency ($0 < f < 0.025$ Hz, VLF) waves to analyse the evolution of these components. The long wave separation was based on the observed frequencies on the reef flat (Figure 3). The peak frequency is considered as the peak frequency offshore, which corresponds to the target peak period T_p of 3.2 s, so the peak frequency is $f_p \approx 0.3125$ Hz.

The hydrodynamics are analysed in the frequency domain by performing Fourier transformations of the surface elevation and flow velocity time series, to obtain an estimate of the variance density spectrum (e.g. Figure 3). Before spectral analysis the stationary part of the raw surface elevation and flow velocity signal is determined to exclude the spin-up and spin-down time of the wave maker and the flume. The stationary part is defined as the period where the ten minute mean and standard

deviation of the signal are constant. This is determined by computing the running ten minute mean and standard deviation over the entire time series. Next, the stationary part of the signal is detrended. The stationary, detrended surface elevation and velocity signal is then Fourier transformed and analysed without any further averaging.

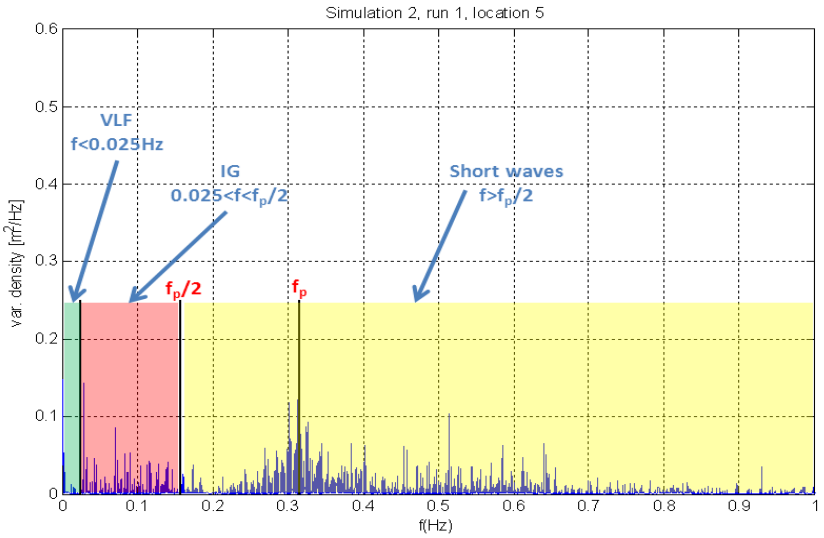

Figure 3. Definition of very low frequency (VLF), infragravity (IG) and short waves used in this paper

The waves were separated into their incoming and reflected components using co-located surface elevation and flow velocity signals following Guza et al. (1984). On the reef flat where the wave height is similar to the water depth, the depth under a wave crest can be double the value of the depth under a trough. Therefore the instantaneous value of h varies strongly and that will affect the propagation velocity c of the waves. To account for these (very) shallow water effects, the water depth in the approach by Guza et al. (1984) was adjusted so that half the observed wave height was added (as proposed by Dingemans (1997)) such that $c = \sqrt{g(h+\zeta)}$ with $\zeta = H/2$.

Third order velocity moment (U^3) decomposition

The third order velocity moment was considered as a proxy for sediment transport on the reef flat and is a measure of skewness in the velocity signal, which will induce sediment transport. Wave skewness is an asymmetry about the horizontal axis with shallower troughs and larger peaks. A positive skewness of the velocity signal results in higher onshore peak velocities and lower, offshore peak velocities. Since sediment transport tends to be proportional to U^3, the higher onshore velocities will induce more transport than the lower offshore velocities, even though the offshore velocity may last longer. Averaging over a wave period results in a proxy for the net transport of sediment. We follow and extend the approach of Roelvink and Stive (1989) to decompose U^3 and investigate the role of long and short waves in sediment transport . The method is discussed in more detail below.

RESULTS

Integral properties of surface elevation and flow

The reflection of wave energy on the reef is significant and varies between 23 and 31% of the incident wave energy. Reflection is slightly higher for the smooth cases when compared to the rough cases as well as for the cases with $h_r = 0.05\ m$ when compared to with $h_r = 0.1\ m$ (Table 2). On the reef flat the reflection is up to 80% (Figure 4), mainly due to long wave reflection and resonance on the reef flat. The resonance or seiching on the reef flat is discussed in more detail further on in this paper.

The rms-values of the flow velocities in the alongshore direction are much smaller than those in cross-shore direction and indicate that there are no cross-tank standing modes present. The experiments are therefore considered one-dimensional.

Table 2. Overview of wave parameters at location 1(offshore, closest to wave maker) for the first part of each run					
Location 1 (offshore)	**R10**	**R05**	**S10**	**S05**	**Target value**
$H_{m0,tot}$ [m]	0.215	0.217	0.216	0.218	-
$H_{m0,i}$ [m]	0.203	0.203	0.204	0.203	0.20
$H_{m0,r}$ [m]	0.048	0.055	0.054	0.062	-
f_p [Hz]	0.322	0.315	0.315	0.322	0.3125
Reflection coefficient: $H_{m0,r}$ / $H_{m0,i}$	0.236	0.271	0.265	0.305	-
T_p [s]	3.105	3.171	3.172	3.105	3.2
T_{m01} [s]	3.335	3.533	3.422	3.616	-
$u_{rms,total}$ [m/s]	0.147	0.154	0.148	0.157	-
$u_{rms,i}$ [m/s]	0.146	0.153	0.146	0.153	-
$u_{rms,r}$ [m/s]	0.041	0.047	0.044	0.052	-
$v_{rms,total}$ [m/s]	0.032	0.029	0.032	0.028	-

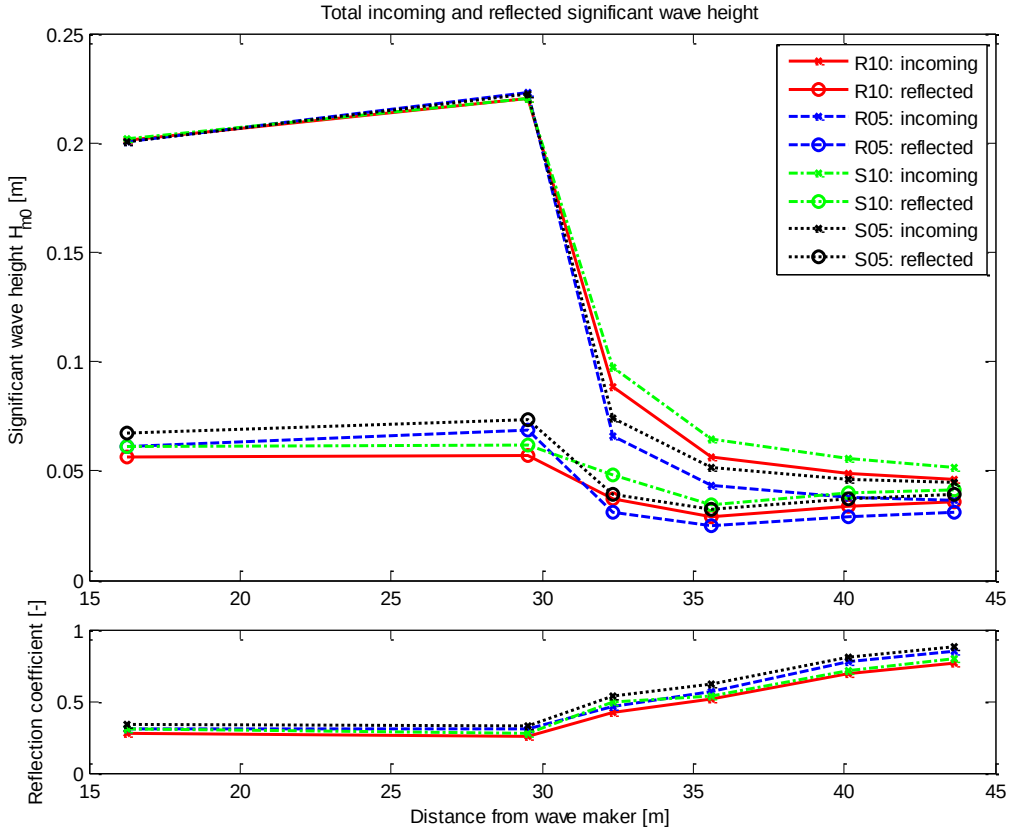

Figure 4. Incoming and reflected total wave height and reflection coefficient for all four cases

Wave transformation

This section discusses the transformation of the short and long waves (IG+VLF) over the reef. Figure 5, upper panel, shows how the total significant wave height H_{m0} transforms along the flume and the reef for long and short waves and for all the different cases. The cross-shore profile of the reef in the flume is shown in the lower panel.

Short waves (SW). Moving from offshore to onshore (Figure 5, upper panel), the significant wave height (H_{m0}) of the short waves (incoming and reflected) increases slightly on the forereef slope because of shoaling. Near the reef crest the short waves break and the wave height drops significantly. At the back of the reef, the short wave height that remains is mainly dependent on the water depth on the reef. The wave height is lower in the two cases with shallow water (S05, R05) than in the cases with deep water (S10, R10).

The short wave height is only slightly affected by the bed roughness elements, as the remaining wave height is lower in the cases with bed roughness compared to the cases without bed roughness. This indicates that there is dissipation of short wave energy on the reef by bottom friction.

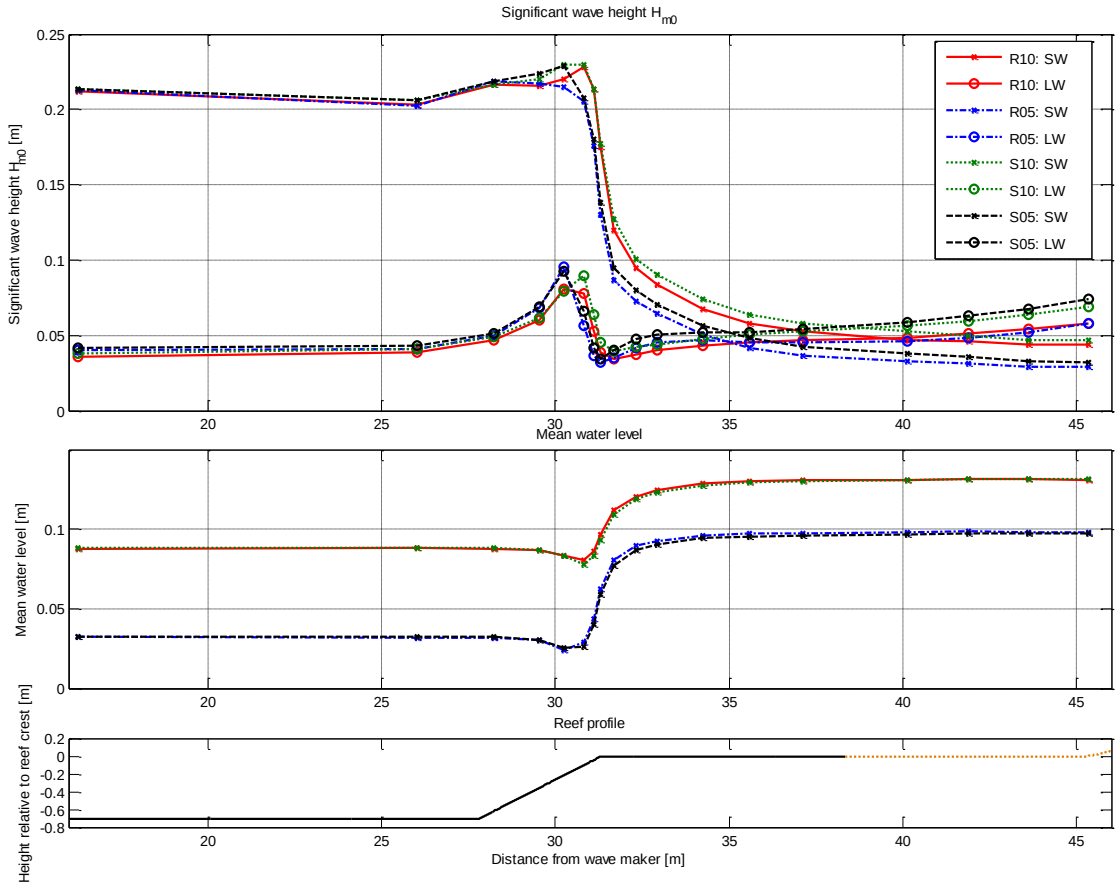

Figure 5. Upper panel: evolution of total significant wave height (H_{m0}) for long and short waves. Compared for all four cases. Middle panel: mean water levels relative to reef crest level. Lower panel: reef profile; the black line indicates the position of the reef; the orange/brown (dashed) line indicates the sand.

Long waves (LW). The significant wave height of the long waves increases strongly on the forereef slope, which is mainly caused by shoaling of long wave energy and some reflection of long wave energy on the reef slope. Near the reef crest the wave height drops significantly and a large part of the long wave energy is dissipated. This dissipation is likely to be caused by depth-induced long wave breaking as discussed by Van Dongeren et al. (2013) based on field observations and modelling of Ningaloo Reef. The increase of long wave energy right after breaking suggests that the waves are generated by the breakpoint mechanism (Symonds et al., 1982). On the reef flat the long wave height increases towards the beach. The largest part of this increase will be shown further on to be caused by a standing wave (seiching) on the reef flat.

The significant long wave height close to the beach and in the lagoon area is higher than the short wave height by 10-40%. Long wave motions are dominant over short wave motions in most of the sandy lagoon area, which is the area where most of the sediment dynamics takes place. This long wave dominance is consistent with observations in the field by Van Dongeren et al. (2013) and Pomeroy et al. (2012).

At the measurement locations close to the beach there is a separation of the long wave height into smooth and rough families as the long wave height for the smooth cases S05 and S10 is higher than for the rough cases R05 and R10. This shows that the long wave height is clearly affected by the bed roughness elements.

Conclusions. There is strong dissipation of wave energy of both long and short waves on the reef crest because of wave breaking. There is some dissipation of short wave energy by bed friction, but this is little small compared to dissipation by wave breaking. The long wave height increases towards the landside of the reef and the long waves are higher than short waves in the lagoon area by about 10-40%. The long wave height at the locations near the beach is observed to be clearly affected by the bed roughness elements.

Wave-induced setup

As a consequence of wave breaking a setup of the mean water level on the reef is induced, according to Eq. 1. The wave forcing, represented as a gradient of the radiation stress $\frac{dS_{xx}}{dx}$, is balanced by a gradient in the mean water level $\rho g h \frac{d\bar{\eta}}{dx}$ and the bed shear stress τ_{bx}^{E}:

$$F_x = -\frac{dS_{xx}}{dx} = \rho g h \frac{d\bar{\eta}}{dx} + \tau_{bx}^{E} = \rho g (h_0 + \bar{\eta}) \frac{d\bar{\eta}}{dx} + \tau_{bx}^{E} \quad (1)$$

The mean value of the water level was determined and plotted in the middle panel of Figure 5. The increase of the mean water level on the reef is quite large in all the cases reaching almost 100% of the initial water level for R05 and S05. The water levels for R10 compared to S10 are equal so for these experiments the increased bed roughness does not affect the setup. Simulation R05 does have a slightly stronger increase of the water level on the reef than S05 and therefore at a lower initial water level on the reef, bed roughness enhances the setup, although its contribution is still close to zero. The fact that the bed roughness has a minimal impact on the setup is counterintuitive. The low impact is due to the low flow velocities on the reef, which do not induce sufficient bed shear stresses to generate a substantial setup of the mean water level.

All four cases show a small, local decrease in water level just before the reef crest. This is where the waves are shoaling so the radiation stress increases causing the observed setdown of the water level. In the offshore region between the wave maker and the reef crest, the water level is decreased with respect to the still water level because of mass conservation in the flume, since the total volume of water is constant.

Table 3 presents the mean water levels relative to the reef crest level that were measured offshore and on the reef. The difference between these values is Δh and should be balanced by the forcing by the breaking waves. Since the water depth on the reef and reef slope is lower in R05 and S05, the effect of (depth-induced) wave breaking is stronger because of the depth term pre-multiplying the pressure gradient, leading to more setup Δh.

Table 3. Mean water levels during the experiments at different locations and the setup Δh. Water levels are relative to reef crest level.

Simulation	SWL [m]	Offshore [m]	Location 15 [m]	Location 18 [m]	Δh [m]
R10	0.10	0.088	0.131	0.131	0.043
R05	0.05	0.031	0.098	0.098	0.067
S10	0.10	0.088	0.131	0.131	0.043
S05	0.05	0.032	0.097	0.097	0.065

Since the reef is modelled in a one-dimensional flume the physics are different from the field where the reef will extend in alongshore direction. The fact that the experiments are one-dimensional leads to relatively high setup compared to an actual reef since the water cannot go anywhere while in reality the water will run off the reef through deeper channels that occur at more or less regular spatial intervals. Still, also in nature significant wave-induced setup occurs on (fringing) reefs where it is an important driving force for flow circulation on the reef (Lowe et al., 2009).

Infragravity waves (IG, 0.025 Hz < f < f_p/2)

The large long wave height on the reef flat near the beach is typical for a fringing reef environment and is further analysed. The variance density spectrum measured on the reef flat shows three distinct peaks that are located in the long wave frequency band (Figure 6).

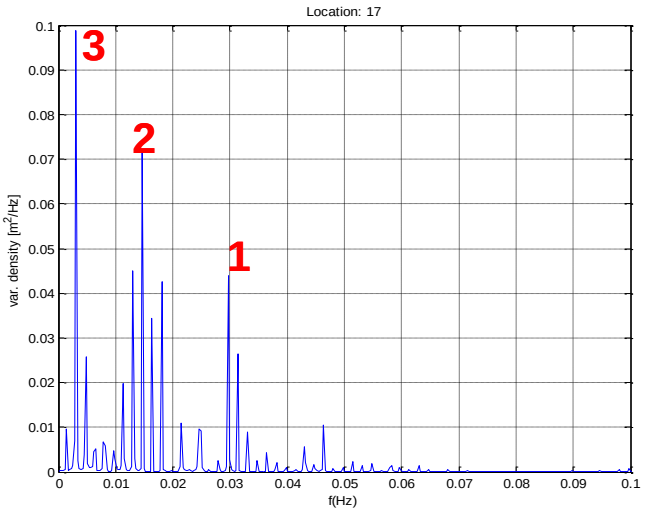

Figure 6. Variance density spectrum of the surface elevation on the reef flat/lagoon at location 17 for simulation R10

Peak number 1 is located around 0.03 Hz (T ~33 s). The peak at this frequency indicates the energy of IG waves, forced by incoming wave groups, which is confirmed by the variance density spectrum of the short wave envelope computed at a location offshore from the reef (Figure 7). The short wave envelope was computed by high pass filtering the measured signal to obtain the short wave (SW) contribution. Of this time series, the Hilbert transform was taken to obtain the envelope time series of which the spectrum was taken (for details, see Van Dongeren et al., 2003). The spectrum thus obtained contains a clear peak around 0.03 Hz. This shows that the group frequency of the incoming short waves corresponds to the IG frequency on the reef and that these IG waves are forced by the incoming short wave groups.

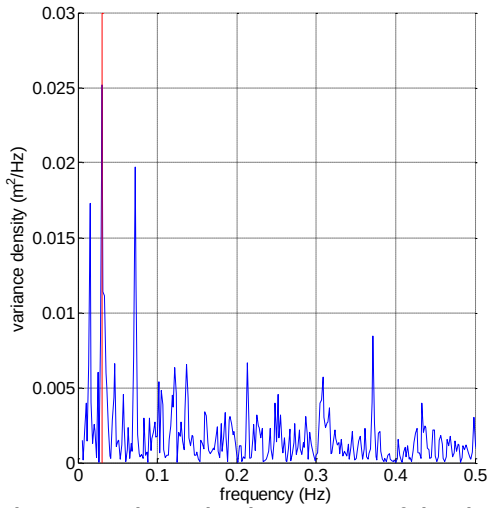

Figure 7. Variance density spectrum of the short wave envelope measured offshore from the reef. The red line indicates a clear peak around 0.03 Hz.

Very Low Frequency motions (VLF, f<0.025 Hz)

The two remaining peaks in the variance density spectrum on the reef flat (2 and 3) are found in the VLF frequency band. Peak number 2 is a consequence of resonance at the eigenfrequency of the reef flat (seiching), which leads to the formation of a standing wave on the reef flat for all four cases. Schematizing the reef flat as a semi-closed basin and computing the theoretical eigenfrequency of this semi-closed basin (e.g. Dean and Dalrymple (1991)) it can be demonstrated that the observed frequency is a result of resonance (seiching) on the reef flat (Table 4).

The computed and observed values of the eigenperiod for all cases are presented in Table 4 and they compare well. The peak that was observed in the spectrum on the reef flat is therefore likely to be caused by resonance at the eigenfrequency of the reef flat. The frequency of the seiching motion is found to depend only on the water depth on the reef (h_r) and not on the bed roughness.

Table 4. Overview of observed and calculated resonance period/frequency for all simulations			
Simulation	Measured period of oscillation [s]	Measured frequency [Hz]	Theoretical eigen period reef flat [s]
R10	65	0.015	56.5
R05	83	0.012	80.0
S10	65	0.015	56.5
S05	83	0.012	80.0

Peak number 3 is an oscillation caused by a very low frequency variation in the offshore short wave energy (T ~300 s), with the source of this peak being further investigated.

Decomposition of the third order velocity moment

The hydrodynamic driving of sediment transport is analysed using the third order velocity moment as a proxy. It can be decomposed to show how long and short wave velocity contribute to the total. The flow velocity can be subdivided into a wave group mean and a time-varying component as follows:

$$u(t) = \bar{u} + \tilde{u}(t) \tag{2}$$

The time-varying component $\tilde{u}(t)$ contains both the variation on the time scale of wave groups and on that of individual waves:

$$\tilde{u} = u_s + u_L \tag{3}$$

The third order velocity moment is defined as: $\langle u|u|^2\rangle$ and is a measure of wave skewness, which is an asymmetry about the horizontal axis with shallower troughs and larger peaks. A positive skewness indicates a landward sediment transport and vice versa for a negative skewness. It is decomposed using a Taylor series expansion and assuming $|\bar{u}| < |\tilde{u}|$ as follows:

$$\langle u|u|^2\rangle \approx \langle \tilde{u}|\tilde{u}|^2\rangle + 3\bar{u}\langle|\tilde{u}|^2\rangle + \bar{u}^3 \tag{4}$$

Where < > denotes time averaging. The term $3\bar{u}\langle|\tilde{u}|^2\rangle$ is the combined contribution of the mean and oscillatory component, the term $\bar{u}^3$ is the contribution of the mean flow and the term $\langle \tilde{u}|\tilde{u}|^2\rangle$ is the contribution of the time-varying component at the time scale ranging from that of wave groups to the individual waves. This time-varying component can be decomposed as follows, using Eq. 3 following Roelvink and Stive (1989) who assumed that $u_L \ll u_s$ and u_s is uncorrelated to $|u_L|^2$ and $|u_L|^3$.

$$\langle \tilde{u}|\tilde{u}|^2\rangle \approx \langle u_s|u_s|^2\rangle + 3\langle u_L|u_s|^2\rangle \; (+3\langle u_s|u_L|^2\rangle + \langle u_L|u_L|^2\rangle) \tag{5}$$

Because of the assumption that $u_L \ll u_s$ the last two terms on the right-hand side drop out of the equation. The two remaining terms on the right-hand side are the short and the long wave contribution to the third order velocity moment and are referred to by Van Dongeren et al. (2007) as:

$\boldsymbol{guss} = \langle u_s|u_s|^2\rangle$ (**short** wave transport and stirring)
$\boldsymbol{guls} = 3\langle u_l|u_s|^2\rangle$ (**long** wave transport, short wave stirring)

By calculating the so-called *guss* and *guls* the contributions of short and long waves to on- or offshore suspended and bed load transport can be assessed. This section looks into the development of the third order velocity moment over the reef flat and extend the decomposition of the time-varying component, $\langle \tilde{u}|\tilde{u}|^2\rangle$, because the assumption that $u_L \ll u_s$ has already been shown to be no longer valid on the reef flat.

Without the assumption that the short wave flow velocity is much larger than the long wave flow velocity the decomposition of the time-varying part of the third order velocity moment contains two extra terms with $|u_L|^2$. The quadratic terms $|u_s|^2$ and $|u_L|^2$ can be interpreted as stirring of sediment by the short and long wave velocity respectively. The total decomposition including long wave stirring becomes:

$$\langle \tilde{u}|\tilde{u}|^2 \rangle = \langle u_s|u_s|^2 \rangle + 3\langle u_L|u_s|^2 \rangle + 3\langle u_s|u_L|^2 \rangle + \langle u_L|u_L|^2 \rangle \quad (6)$$

Besides the guss and guls two new terms appear which are named in the same manner which was also described by Rocha et al. (2013) for a different case:

$\boldsymbol{gusl} = 3\langle u_s|u_L|^2 \rangle$ (short wave transport, long wave stirring)
$\boldsymbol{gull} = \langle u_L|u_L|^2 \rangle$ (long wave transport and stirring)

The development of the time-varying components of the total third order velocity moment over the reef is presented in Table 5. The values at location 15 and 17 are of particular interest, because these are on the sandy bed of the lagoon. The values are all positive and decrease strongly from location 10 at the reef crest to location 13, 15 and 17 close to and on the sandy lagoon. The values decrease slightly from 13 to 15 and remain more or less constant from 15 to 17, except for case S05.

Table 5. Total third order velocity moment at the four reef locations and all cases.

$\boldsymbol{total} = \langle \tilde{\boldsymbol{u}}|\tilde{\boldsymbol{u}}|^2 \rangle * \boldsymbol{10^{-2}}$	10	13	15	17
R10	0.85	0.114	0.078	0.077
R05	0.75	0.099	0.093	0.10
S10	1.67	0.14	0.10	0.11
S05	1.39	0.20	0.145	0.18

The evolution of the different components over the reef flat is presented in Figure 8. It is clear that for the experiments the assumption of $u_L \ll u_s$ is no longer valid since in all cases the long wave component *gull* becomes the dominant component of the third order velocity moment near the beach. The relative contribution of the *gull* is largest for the cases with a low water depth (S05 and R05) since the remaining short wave velocity in those cases is relatively small because of depth-induced breaking of the short waves. Also in the deeper water cases (S10 and R10) the contribution of the *gull* is dominant at the end of the lagoon, but in those cases the contribution related to the short wave stirring, which is the sum of the *guss* and *guls*, remains more important as these terms together (red and blue line) are the largest contribution to the velocity moment.

Bed roughness reduces the contribution of the long wave component *gull*, comparing R10 to S10 and R05 to S05, which is in agreement with observations of the long wave height being smaller in the cases with bed roughness.

As discussed in the previous chapter, the VLF motions contribute significantly to the long wave energy on the reef. This contribution is included in the long wave flow velocity in the above analysis and particularly makes up a large part of the *gull* component.

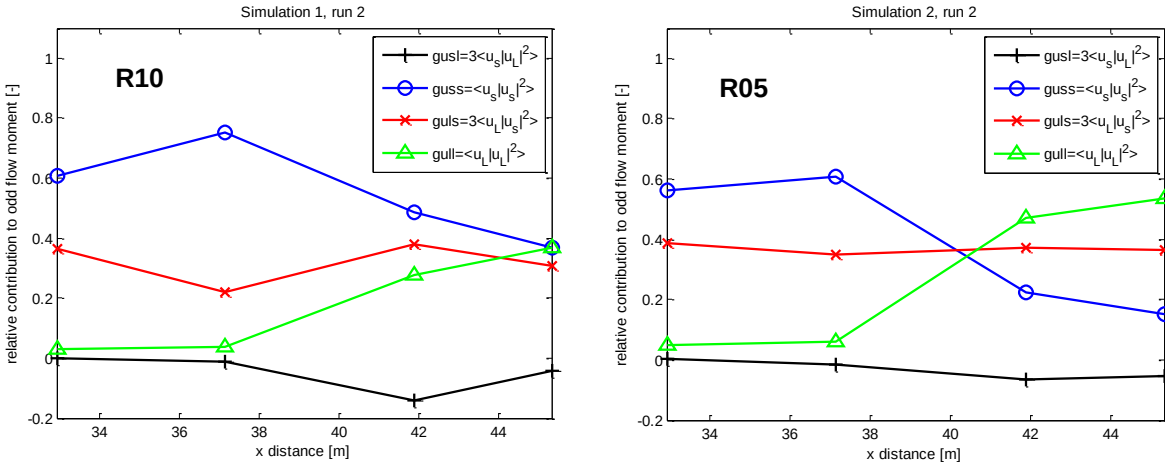

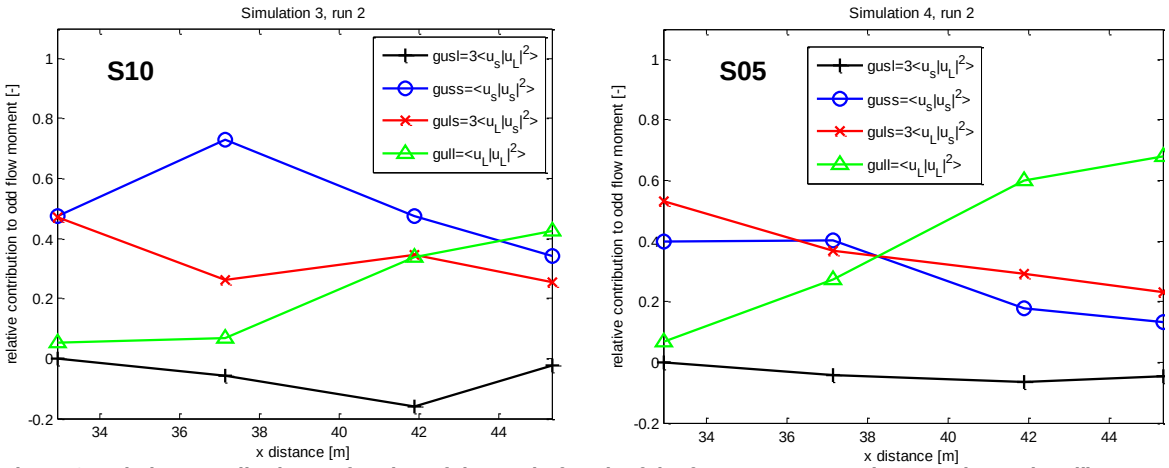

Figure 8. Relative contribution as fraction of the total of each of the four components (guss, guls, gusl, gull) to the total third order velocity moment and the evolution over the reef.

DISCUSSION

Implications for sediment dynamics

The results of the development of the third order velocity moment over the reef flat are used to investigate how the hydrodynamics drive sediment transport. Table 5 shows that the values at all locations and for all cases are positive so that would indicate a trend of landward transport by the time-varying components in the velocity moment. Since in all cases the long wave component *gull* becomes the dominant contributing component to the third order velocity moment near the beach (Figure 8), it can be expected that the sediment transport in the lagoon is caused for a large portion by the long waves through long wave stirring and advection.

In the cases with a low water depth (S05 and R05) the long wave contribution *gull* is larger than the short wave contribution, showing that long waves play the dominant role in sediment transport in this region. In the deeper water cases (S10 and R10) the long wave contribution *gull* is also large at the end of the lagoon, but it is of similar magnitude as the short wave contributions, indicating that both long and short waves play a role in sediment transport in these cases. The long wave contribution to sediment transport is slightly smaller for the rough cases (R05 and R10) compared to the smooth cases (S05 and S10).

The results of this analysis are influenced by the presence of the VLF motions which account for a significant part of the long wave flow velocity u_L and therefore they contribute to the transport of sediment on the reef flat and in the lagoon.

Also, the analysis only considered the time varying part of the third order velocity moment and not the contribution of the mean flow. The contribution of the mean flow is significant, because of the (offshore directed) undertow. It was found that the mean flow contribution induces offshore directed sediment transport, but that the total third order velocity moment has an increasing trend and that it is positive in the lagoon area, indicating onshore transport (Bodde, 2013).

Resulting bed profile development

The decomposition and analysis of the third order velocity moments showed that on average there is onshore directed sediment transport and that there is a significant contribution of the long waves to the total sediment transport on the reef and in the lagoon. Below we discuss how this is reflected in sediment transport during a complete simulation, by assessing the bed profile development in the lagoon area.

Bed profile measurements were performed before each simulation and after one, three and seven hours. The measurements at the start of a simulation and after 7 hours are shown in Figure 9 for all cases. The profile developments look similar for both simulations with a lowering of the bed level at the start of the lagoon (x=38-40 m) and an increase of the bed level in the remaining part of the lagoon (x=40-45 m), indicating onshore transport of sediment. Also a steepening of the beach slope is observed and the formation of a swash bar at a height of about 0.25 m.

There are two clear differences between the S10 (smooth) and the R10 (rough) case. The first one is in the shape of the swash bar which seems to be more pronounced and located higher up the slope for the smooth case and secondly the lowering of the bed level at the start of the lagoon appears to be slightly stronger in the smooth case.

Both differences are likely to be an effect of the larger long wave height and corresponding flow velocity in the lagoon and higher run-up for the smooth cases. The flow velocity at the onset of the lagoon is higher in the smooth case causing more clear-water scour at the transition from hard reef to the sandy lagoon. At the beach the long waves are higher for case S10 increasing the intensity with which the swash bar is developed. It is suggested to relate these observations to the run-up measurements that were done during the hydrodynamic part of the experiments (Buckley et al., in prep).

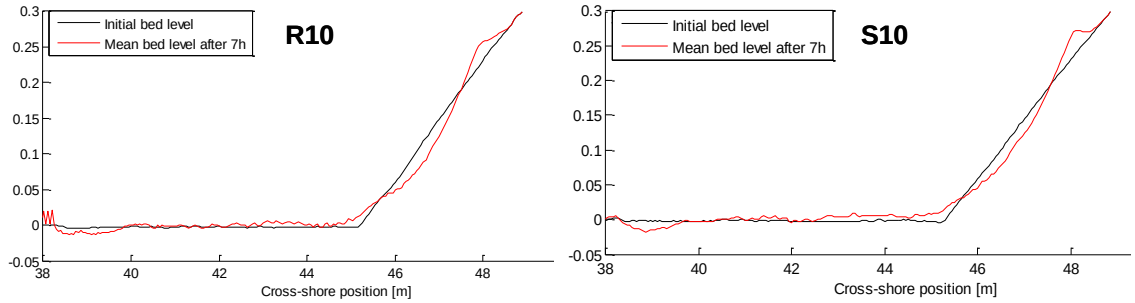

Figure 9. Profile development after a run for a rough and a smooth case

CONCLUSIONS

Hydrodynamics

Roughness and water level in a fringing reef environment were shown to have an influence on many processes such as short wave breaking, infragravity (IG) wave transformation, seiching, wave-induced setup and wave reflection. Analysis of the wave transformation over the reef of long and short waves confirmed the importance of long waves on a fringing coral reef as it showed that they become dominant towards the lagoon and beach. Near the beach it was found that the short waves are controlled by water depth, because of depth-induced breaking, and the total long wave height is controlled by bed roughness. At the measurement locations close to the beach there is a separation of the long wave height into smooth and rough families as the long wave height for the smooth cases S05 and S10 is higher than for the rough cases. This shows that the long wave height is clearly affected by the bed roughness elements.

The mean water levels were used to determine the wave-induced setup and setdown. The water level on the reef was almost double the initial water level h_r for simulation R05 and S05 and confirmed the importance of setup on fringing reefs (e.g. Lowe et al., 2009). The setup was largest for these simulations because of stronger wave forcing and a smaller water column on which the forcing was active. The effect of bed friction on the setup was negligible comparing R10 and S10, and gave a very minor contribution to the setup for case R05. This may be counter to intuition but is due to the low flow velocities, which appear to not induce sufficient bed shear stress to affect the setup significantly.

It was observed that the total long wave energy increases towards the beach which is caused by resonance at the eigenfrequency of the reef flat and the flume and reflection of progressive waves on the beach slope. The long waves were separated into an IG range ($0.025<f<f_p/2$ Hz) and a very low frequency, or VLF, range ($0<f<0.025$ Hz) for further analysis. IG waves at a frequency of about 0.03 Hz were found to be forced by the incoming short wave groups. The VLF range included two peaks in the spectrum which were analysed: a standing wave with a period in the order of 60-80 seconds and a long period motion of 330 seconds. The presence of a standing wave was confirmed by the increase of the long wave height towards the beach. The observed frequencies of the standing waves agreed quite well with theoretical values of the eigenfrequency of the reef and the flume and varied with depth.

Sediment dynamics

The third order velocity moment is considered as a proxy for sediment transport. The analysis of the third order velocity moment relates the hydrodynamics to sediment transport. It shows that the long wave contribution to sediment stirring and transport becomes important close to the beach and that there is a trend of onshore transport. The results are consistent with the fact that long waves are dominant in the lagoon in this study.

Bed roughness reduces the contribution of the long wave component *gull*, which is in agreement with observations of the long wave height being smaller in the cases with bed roughness. In the deep water cases (R10 and S10) the contribution of the *gull* is dominant at the end of the lagoon. Still, in those cases the transport related to the short wave stirring (*guss+guls)* remains more important as these

terms together are the largest contribution to the velocity moment. In the shallow water cases the long wave contribution *gull* is larger than the short wave contribution, showing that long waves are the dominant factor in sediment transport due to wave skewness.

The contribution of the time-varying part to the total third order velocity moment is positive, indicating onshore directed transport. Combined with the bed profile developments this paints a very consistent picture in which both the short and the long waves play a role, but the long waves appear to be the dominant factor in sediment transport and bed profile development especially close to the beach. Also an effect of the roughness elements is observed in the bed profile development, mainly in the shape of the swash bar, which is different for rough and smooth cases.

This shows that the clear presence of long waves in a fringing reef lagoon indeed results in different sediment dynamics than for example on a regular sandy beach. It can be concluded that the specific hydrodynamic drivers in a fringing reef environment are reflected in the sediment transport and in the bed profile development.

ACKNOWLEDGMENTS

The laboratory experiment forms part of a PhD study by A. Pomeroy and is supported by a Robert and Maude Gledden Postgraduate Research Award and The Gowrie Trust Fund. The experiment was funded by an ARC Future Fellowship Grant to R. Lowe and a UWA Research Collaboration Award to A. Pomeroy and R. Lowe. This work was funded in part by Deltares Strategic Research in the Event-driven Hydro- and Morphodynamics program (project number 1209342). Additional funding was provided by Witteveen+Bos.

REFERENCES

Baldock, T.E. (2012). Dissipation of incident forced long waves in the surf zone—Implications for the concept of "bound" wave release at short wave breaking. *Coastal Engineering, 60*(0), 276-285. doi: 10.1016/j.coastaleng.2011.11.002

Bodde, W.P. (2013). *Sediment transport in a fringing reef environment: Analysis using laboratory experiment and numerical modelling.* MSc Thesis, TU Delft, Delft.

Dean, R., & Dalrymple, R. (1991). Water wave mechanics for scientists and engineers. *World Sci entific, Advanced Series on Ocean Eng, 2*.

Ferrario, F., Beck, M. W., Storlazzi, C. D., Micheli, F., Shepard, C. C., & Airoldi, L. (2014). The effectiveness of coral reefs for coastal hazard risk reduction and adaptation. *Nature communications*, *5*.

Hearn, C.J. (1999). Wave-breaking hydrodynamics within coral reef systems and the effect of changing relative sea level. *Journal of Geophysical Research, 104*(C12), 30007-30019.

Holthuijsen, L. H. (2007). *Waves in oceanic and coastal waters*. Cambridge University Press.

Komar, P. (1998). *Beach Processes and Sedimentation* (2nd ed.). Upper Saddle River, N.J.: Prentice-Hall.

Lee, T.T., & Black, K.P. (1978). *The energy spectra of surf waves on a coral reef.* Paper presented at the Proceedings of the International Conference on Coastal Engineering.

Longuet-Higgins, M. S., & Stewart, R. W. (1962). Radiation stress and mass transport in gravity waves, with application to 'surf beats'. *Journal of Fluid Mechanics*, *13*(04), 481-504.

Longuet-Higgins, M. S., & Stewart, R. W. (1964). Radiation stresses in water waves; a physical discussion, with applications. In *Deep Sea Research and Oceanographic Abstracts* (Vol. 11, No. 4, pp. 529-562). Elsevier.

Lowe, R.J., Falter, J.L., Bandet, M.D., Pawlak, G., Atkinson, M.J., Monismith, S.G., & Koseff, J.R. (2005). Spectral wave dissipation over a barrier reef. *Journal of Geophysical Research, 110*(C4), C04001.

Lowe, R.J., Falter, J.L., Koseff, J.R., Monismith, S.G., & Atkinson, M.J. (2007). Spectral wave flow attenuation within submerged canopies: Implications for wave energy dissipation. *Journal of geophysical research, 112*(C5), C05018.

Lowe, R. J., Falter, J. L., Monismith, S. G., & Atkinson, M. J. (2009). Wave-driven circulation of a coastal reef-lagoon system. *Journal of Physical Oceanography*, *39*(4), 873-893.

Lowe, R. J., & Falter, J. L. (2014). Oceanic Forcing of Coral Reefs. *Annual Review of Marine Science*, *7*(1).

Monismith, S. G. (2007). Hydrodynamics of coral reefs. *Annu. Rev. Fluid Mech.*, *39*, 37-55.

Munk, W.H., & Sargent, M.C. (1948). Adjustment of Bikini Atoll to ocean waves. *Trans. Am. Geophys. Union, 29*, 855-860.

Pomeroy, A., Lowe, R., Symonds, G., Van Dongeren, A., & Moore, C. (2012). The dynamics of infragravity wave transformation over a fringing reef. *Journal of Geophysical Research: Oceans (1978–2012), 117*(C11).

Roelvink, D., Reniers, A., Van Dongeren, A., Van Thiel De Vries, J., Mccall, R., & Lescinski, J. (2009). Modelling storm impacts on beaches, dunes and barrier islands. *Coastal Engineering, 56*(11), 1133-1152.

Roelvink, D., & Stive, M. (1989). Bar-generating cross-shore flow mechanisms on a beach. *J. Geophys. Res, 94*(C4), 4785-4800.

Rocha, M.V., Michallet, H., Silva, P.A., Abreu, T., & Barthélemy, E. (2013). Nonlinearities of short and long waves across the shoaling, surf and swash zones: Physical model results. *Proceedings Coastal Dynamics 2013*.

Storlazzi, C.D., Field, M.E., Bothner, M.H., Presto, M., & Draut, A.E. (2009). Sedimentation processes in a coral reef embayment: Hanalei Bay, Kauai. *Marine Geology, 264*(3), 140-151.

Symonds, G., Huntley, D.A., & Bowen, A.J. (1982). Two-Dimensional Surf Beat: Long Wave Generation by a Time-Varying Breakpoint. *Journal of Geophysical Research, 87*(C1), 492-498.

Van Dongeren, A.R., A.J.H.M. Reniers, J.A. Battjes and I.A. Svendsen (2003). Numerical modeling of infragravity wave response during Delilah. *Journal of Geophysical Research*, 108, (C9), 3288, doi:10.1029/2002JC001332.

Van Dongeren, A., Lowe, R., Pomeroy, A., Trang, D.M., Roelvink, D., Symonds, G., & Ranasinghe, R. (2013). Numerical modeling of low-frequency wave dynamics over a fringing coral reef. *Coastal Engineering, 73*, 178-190. doi: 10.1016/j.coastaleng.2012.11.004

Van Dongeren, A., Wenneker, I., Roelvink, D., & Rusdin, A. (2007). A Boussinesq-type wave driver for a morphodynamical model. *Proceedings of the Coastal Engineering Conference*, 3129-3141.

Young, I.R. (1989). Wave transformation over coral reefs. *Journal of Geophysical Research, 94*(C7), 9779-9789.